MOLECULAR AND CELLULAR BIOLOGY, May 2008, p. 2908–2919 Vol. 28, No. 9
0270-7306/08/$08.00+0 doi:10.1128/MCB.02065-07

Presenilin 1 Interacts with Acetylcholinesterase and Alters Its Enzymatic Activity and Glycosylation▽

María-Ximena Silveyra,[1,2] Geneviève Evin,[3,4] María-Fernanda Montenegro,[6] Cecilio J. Vidal,[6] Salvador Martínez,[1] Janetta G. Culvenor,[3,4,5] and Javier Sáez-Valero[1,2]*

Instituto de Neurociencias de Alicante, Universidad Miguel Hernández-CSIC, Sant Joan d'Alacant E-03550, Spain[1]; Centro de Investigación Biomédica en Red Sobre Enfermedades Neurodegenerativas, Madrid, Spain[2]; Department of Pathology, The University of Melbourne, Melbourne, Victoria 3010, Australia[3]; The Mental Health Research Institute of Victoria, Parkville, Victoria 3052, Australia[4]; The Centre for Neuroscience, The University of Melbourne, Melbourne, Victoria 3010, Australia[5]; and Departamento de Bioquímica y Biología Molecular-A, Universidad de Murcia, Murcia E-30071, Spain[6]

Received 16 November 2007/Returned for modification 18 January 2008/Accepted 14 February 2008

Presenilin 1 (PS1) plays a critical role in the γ-secretase processing of the amyloid precursor protein to generate the β-amyloid peptide, which accumulates in plaques in the pathogenesis of Alzheimer's disease (AD). Mutations in PS1 cause early onset AD, and proteins that interact with PS1 are of major functional importance. We report here the coimmunoprecipitation of PS1 and acetylcholinesterase (AChE), an enzyme associated with amyloid plaques. Binding occurs through PS1 N-terminal fragment independent of the peripheral binding site of AChE. Subcellular colocalization of PS1 and AChE in cultured cells and coexpression patterns of PS1 and AChE in brain sections from controls and subjects with sporadic or familial AD indicated that PS1 and AChE are located in the same intracellular compartments, including the perinuclear compartments. A PS1-A246E pathogenic mutation expressed in transgenic mice leads to decreased AChE activity and alteration of AChE glycosylation and the peripheral binding site, which may reflect a shift in protein conformation and disturbed AChE maturation. In both the transgenic mice and humans, mutant PS1 impairs coimmunoprecipitation with AChE. The results indicate that PS1 can interact with AChE and influence its expression, supporting the notion of cholinergic-amyloid interrelationships.

Alzheimer's disease (AD) is characterized by the presence of large numbers of amyloid plaques and neurofibrillary tangles in the brain (56). The major constituent of the amyloid plaques is the β-amyloid protein (Aβ), a polypeptide generated by processing of a much larger amyloid precursor protein (APP) through the successive action of two proteolytic enzymes, β-secretase and γ-secretase (71). γ-Secretase is a membrane protease complex comprising presenilin 1 (PS1) as a catalytic subunit (76). The importance of PS was first highlighted by genetic studies of AD. Families bearing mutations in the PS1 gene, or in the highly homologous presenilin 2 (PS2) gene, invariably develop an aggressive form of early-onset AD with an accelerated rate of Aβ deposition (75).

The accumulation of Aβ peptide in the brain is thought to be an important step in the pathogenesis of AD, leading to a number of neurodegenerative changes (19). In particular, there is a decrease in cholinergic activity in the basal forebrain of AD patients, which affects activity of the acetylcholine-synthesizing enzyme, choline acetyltransferase, as well as the acetylcholine-hydrolyzing enzyme, acetylcholinesterase (AChE) (13, 53). The altered expression of AChE in the AD-affected brain (AD brain) is of particular interest. Despite an overall decrease in the AD brain, the activity of AChE is increased around the amyloid plaques (42, 78). This may be a direct consequence of amyloid deposition, since Aβ peptides influence AChE levels in cell cultures (25, 69) and in the brains of transgenic mice that produce human Aβ (70). Conversely, AChE may play a role in Aβ fibrillogenesis (27, 60). Finally, several investigations have argued for a strict interrelation between amyloid processing and AChE activity. Cholinergic mechanisms modulate amyloid metabolism (49, 63), and AChE inhibitors affect APP processing (32, 43, 82). Although these findings support the notion of cholinergic-amyloid interrelationships, the possibility of an interaction between AChE and PS1 has not yet been explored.

To test the hypothesis that PS1 may interact with AChE, we performed coimmunoprecipitation experiments with human brain extracts. The subcellular colocalization of PS1 and AChE was examined in COS-7 cells in order to corroborate a functional interaction between the two proteins. The distribution of both proteins was also investigated in normal and AD brain, including familial AD (FAD)-associated PS1 variants, by immunohistochemistry. We also explored whether the binding affinity of PS1 for AChE and its molecular forms changed in the diseased brain. Finally, we investigated whether PS1 mutations could affect AChE expression in a transgenic mouse model.

MATERIALS AND METHODS

Collection of brain samples. Samples from age-matched controls (nondemented controls [NDC]) corresponded to cases with no cognitive impairment or symptoms of any neurodegenerative disease and not in acute phases of stroke or inflammatory brain disease (ratio, four male/four female; median age, 61 years [range, 42 to 76 years]). AD cases were selected on the basis of their clinical

* Corresponding author. Mailing address: Instituto de Neurociencias de Alicante, Universidad Miguel Hernández-CSIC, Crta. Alicante-Valencia Km.87, Sant Joan d'Alacant E-03550, Spain. Phone: 34 965919580. Fax: 34 965919561. E-mail: j.saez@umh.es.

▽ Published ahead of print on 25 February 2008.

history of dementia, neuropathological study, and genomic analysis. None of the cases selected had received cholinesterase inhibitor treatment during their last year of life. After neuropathological examination, sporadic AD cases were categorized as stages VI of Braak and Braak (5) (ratio, six male/five female; median age, 72 years [range, 61 to 87 years]). Despite the definition of an AD group composed of sporadic cases, four FAD brains from affected subjects bearing PS1-V89L (two cases, one male, 54 years old, stage V; one male, 57 years old, stage VI [59]), M139T (one male, 64 years old, stage V [6]), and E318G (one male, 54 years old, stage IV [1]) mutations were also grouped and utilized in the study. It should be noted that controversy exists on the causal relationship of PS1-E318G with FAD (1, 41). E318G-PS1 expression, however, is associated with increased production of Aβ42 (44) and neuronal cell death (23), indicating that E318G-PS1 has the same biological potential as other FAD-linked mutants of PS1. Four human embryonic brains from an ~22-gestational-week-old fetus were also analyzed in the present study. Adult brains were from the Banc de Teixits Neurològics, Universitat de Barcelona-Hospital Clínic (Barcelona, Spain), and nonpathological embryonic tissue from the Banc de Teixits Fetals of the Hospital Vall d'Hebron (Barcelona, Spain).

Preparation of brain extracts. Pieces (0.1 g) of human frontal cortex (NDC and AD) and cortices of mice (control and transgenic) stored at −80°C were thawed slowly at 4°C and homogenized (10% [vol/vol]) in 50 mM Tris-HCl (pH 7.4)–500 mM NaCl–5 mM EDTA–1% (wt/vol) Nonidet P-40–0.5% (wt/vol) Triton X-100 (buffer A) and supplemented with a cocktail of protease inhibitors (66). The homogenates were sonicated and centrifuged at 70,000 × *g* at 4°C for 1 h, and the supernatants were collected and frozen at −80°C until assay.

Enzymatic assay and protein determination. AChE activity was assayed as reported elsewhere (66) by using 50 μM tetraisopropyl pyrophosphoramide (Iso-OMPA) as an inhibitor of butyrylcholinesterase, an enzyme that coexists with AChE in human brain and other tissues. One milliunit of AChE activity was defined as the number of nanomoles of acetylthiocholine hydrolyzed per minute at 22°C. Total protein concentrations were determined by using the bicinchoninic acid method (Pierce).

Antibodies. Rabbit antibodies were raised to amino acids 1 to 20 of the PS1 N-terminal fragment (PS1-NTF; antibody 98/1) or the 301 to 317 loop region of PS1 (antibody 00/2; see reference 16). The goat polyclonal anti-AChE antibody N-19, the goat polyclonal anti-AChE antibody E-19, and the horseradish peroxidase (HRP)-conjugated donkey anti-goat immunoglobulin G (IgG) antibody were purchased from Santa Cruz Biotechnology. The goat polyclonal anti-AChE antibody ab31276 was from Abcam, Plc., and the monoclonal antibody MA3-042 (clone HR2) was from ABR-Affinity BioReagents. HRP-conjugated goat anti-rabbit IgG antibody was from Sigma-Aldrich Co. Alexa Fluor 488-labeled goat anti-mouse IgG and Alexa Fluor 555-labeled donkey anti-rabbit IgG were from Invitrogen.

Immunoprecipitations and Western blot analysis. Brain extracts were precleared by incubation with protein A-Sepharose (Amersham Pharmacia) for 2 h at 4°C. Immunoprecipitations were done at 4°C by incubating overnight 800 μg of the proteins with primary antibodies (98/1 or MA3-042) previously coupled to protein A-Sepharose by using dimethyl pimelimidate dihydrochloride (Sigma-Aldrich). Precipitated proteins were washed twice with Tris-buffered saline–0.1% Triton X-100 and once with Tris-buffered saline and were eluted by 0.1 M glycine buffer (pH 2.5). After centrifugation and pH neutralization, supernatants were boiled in Laemmli sample buffer for 10 min and subjected to sodium dodecyl sulfate-polyacrylamide gel electrophoresis (SDS-PAGE), and separated proteins were transferred to nitrocellulose membranes (Schleicher & Schuell Bioscience GmbH). Blots were incubated with anti-AChE N-19 (1:200 dilution), anti-PS1 98/1 (1:2,000 dilution), or anti-PS1 00/2 (1:1,000 dilution). Western blotting using enhanced chemiluminescence detection was performed according to the manufacturer's instructions (Amersham Pharmacia).

AChE affinity matrix. Fasciculin is a polypeptide toxin from snake venom that binds AChE with high affinity through its peripheral site (4, 47). The binding of brain AChE to immobilized fasciculin-2 (Fas2-Sepharose), prepared as described previously (47) (50 μl of matrix and 0.1 ml of sample, dilution to 1:5 in 10 mM Tris-HCl [pH 7.5]), was tested by incubation overnight at 4°C. Bound proteins were washed and reserved with the unbound fraction for Western blot analysis.

Immunocytochemistry. COS-7 cells plated on poly-L-lysine-coated slide glasses were fixed with 4% paraformaldehyde–4% sucrose in phosphate-buffered saline (PBS) for 30 min at 37°C. The cells were incubated overnight at 4°C with primary antibodies diluted in blocking solution (2% goat antiserum 2% bovine serum albumin in PBS containing 0.1% Triton X-100). Double immunostaining was performed with anti-PS1 NTF antibody 98/1 (1:800) and monoclonal anti-AChE antibody MA3-042 clone HR2 (1:200) as primary antibodies and Alexa Fluor 488-labeled goat anti-mouse IgG or Alexa Fluor 555-labeled donkey anti-rabbit IgG (Invitrogen) as secondary antibodies. Dual immunofluorescence images were captured with sequential scans using a Leica laser-scanning spectral confocal microscope (TCS SL; Leica Microsystem). Images were digitized and adjusted by using Adobe Photoshop software (Adobe Systems). Human frontal cortex sections (20 μm thick) were obtained in a freezing microtome (Leica). Double-label immunohistochemistry used anti-PS1 NTF antibody 98/1 (1:8,000), HRP-goat anti-rabbit antibody (Dako) as a secondary antibody, and development with carbiozamine solution (4 mg of AEC [3-amino-9-ethylcarbazole]/ml; Sigma-Aldrich) in dimethyl formamide (Sigma-Aldrich) (57). Slides were mounted in glycerol (20% in PBS) and photographed. The red precipitate was then completely removed by several washes in 70% ethanol, and the second reaction was initiated using anti-AChE antibody MA3-042 (1:200), HRP-goat anti-mouse antibody, and development with a classical 3,3′-diaminobenzidine (DAB)–Tris-HCl solution (Sigma-Aldrich). To ensure that no reactive HRP product from the first antibody remained for the second immunoreaction, sections were blocked for the HRP activity by washing slides in 3% H_2O_2 solution (10 min), and control sections were also incubated directly with DAB solution to check that no signal from the first reaction was still present. Sections were then mounted with glycerol, and the same fields were photographed. Finally, cresyl violet staining was performed for several slides from each case, after the DAB reaction, before coverslips with Eukitt were added and subsequent analysis.

Sedimentation analysis. The molecular forms of AChE were separated according to their sedimentation coefficients by ultracentrifugation at 150,000 × *g* in a continuous sucrose gradient (5 to 20% [wt/vol]) containing 0.5% (wt/vol) Triton X-100 for 18 h at 4°C.

PS1A246E transgenic mice and Western blot analysis for AChE. Mice expressing the human PS1A246E gene under the control of human Thy-1 promoter were used (58). Transgenic mice derived from the line 16-3 PS1A246E, on a C57BL/6/SJL background, were used. Wild-type C57BL/6/SJL mice were used as controls. Equal amount of proteins (brain cortical extracts) were resolved by Western blotting. The strips were incubated with anti-AChE E-19 (1:200 dilution). For semiquantitative analysis, protein levels were normalized to α-tubulin, and the intensity of the bands was measured by densitometry with Science Lab Image Gauge v4.0 software provided by Fujifilm.

Semiquantitative PCR assay for AChE RNA. PS1A246E mouse brain AChE mRNAs were identified by reverse transcriptase PCR (RT-PCR) with selected primers. First-strand cDNAs were obtained by reverse transcription using SuperScript III RT (Invitrogen Life Technologies) according to the manufacturer's instructions using 1 μg of total RNA and oligo$(dT)_{12\text{-}18}$. This assay consisted essentially of the methodology reported elsewhere (20). All cDNAs were normalized to GAPDH (glyceraldehyde-3-phosphate dehydrogenase).

Lectin-binding analysis of AChE. Aliquots of brain extracts were mixed with immobilized *Lens culinaris* agglutinin (LCA; Sigma-Aldrich). After overnight incubation at 4°C, AChE-lectin complexes were separated from free AChE by centrifugation. The unbound AChE activity was evaluated in the supernatant fraction, the bound AChE species were assayed by Western blotting, and both fractions were used to compare differences in lectin binding among groups.

Statistical analysis. All data were analyzed using SigmaStat (version 2.0; SPSS, Inc.) by using the Student *t* test (two-tailed) or by one-way analysis of variance, followed by the Student *t* test for single pairwise comparisons. The results are presented as means ± the standard error of the mean. *P* values of <0.05 were considered significant.

RESULTS

Coimmunoprecipitation of PS1 with AChE from human brain embryonic extracts. Considering that PS1 is expressed at high levels in embryonic brain compared to mature brain (34), we used human embryonic cortex (22 gestational weeks) to examine a possible interaction between PS1 and AChE. PS1 is known to undergo endoproteolytic cleavage as part of its maturation, generating N- and C-terminal derived fragments (54, 77), and extraction with Triton X-100 causes dissociation of these PS1 constituent subunits (7). Thus, we performed immunoprecipitation and Western blotting with PS1 antibodies directed to each fragment. Human embryonic brain cortex samples (prepared in the presence of 1% [wt/vol] Nonidet P-40–0.5% [wt/vol] Triton X-100) were first immunoprecipi-

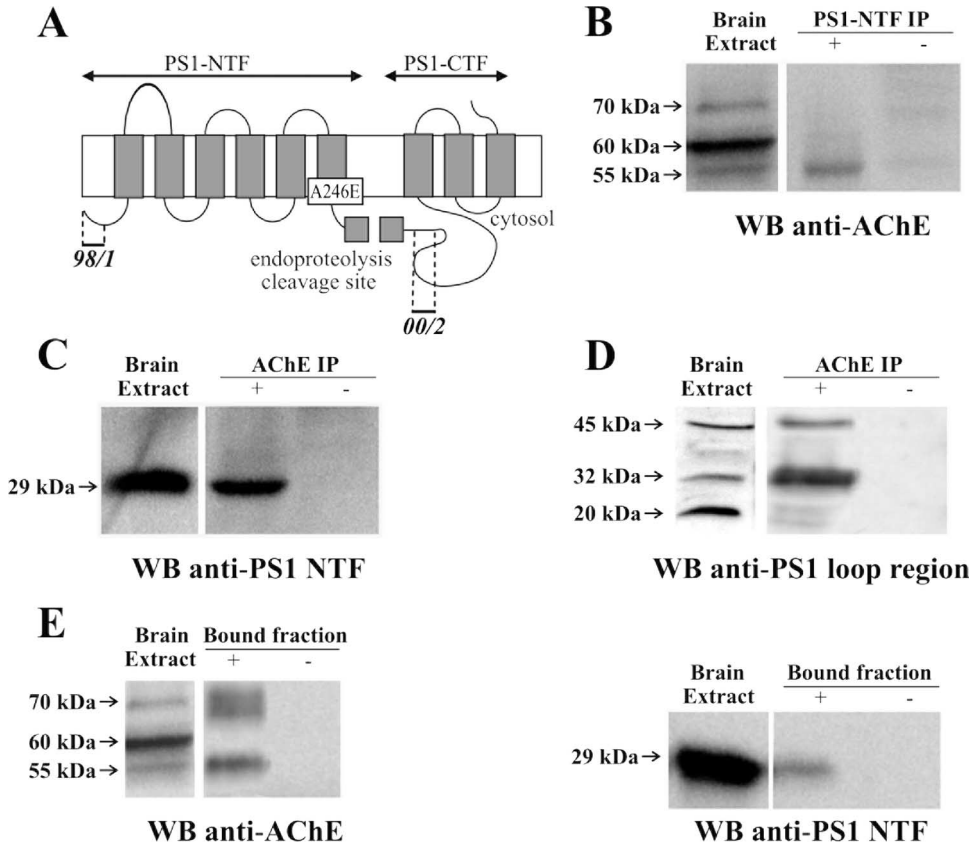

FIG. 1. Coprecipitation of PS1 and AChE. (A) Schematic representation of PS1 nine-transmembrane domain structure and epitopes for 98/1 and 00/2 antibodies. The position of the A246E mutation is indicated. (B to D) Human embryonic brain extracts (~22-gestational-week-old fetus) were immunoprecipitated with anti-PS1 98/1 antibodies (B) or anti-AChE MA3-042 antibodies (C and D). Precipitated proteins were immunoblotted with the indicated antibody. Extracts incubated with protein A-Sepharose, with omission of the antibody, were analyzed in parallel as negative controls. (E) Brain extracts were incubated with immobilized Fas2. The bound fraction was analyzed by Western blotting with N-19 and 98/1 antibodies. Fas2-Sepharose in the absence of brain extract was the negative control.

tated using 98/1 antibody, which recognizes PS1-NTF (see Fig. 1A) (16). We estimated that ca. 13% ± 2% ($n = 4$) of AChE activity was pulled down from the supernatant fraction.

As expected from a prior report (21), Western blot analysis with anti-AChE antibody N-19 detected a complex AChE banding-pattern, with a 55-kDa band detected in PS1 immunoprecipitates (Fig. 1B). This band was not observed in negative immunoprecipitation controls, including omission of the 98/1 antibody (Fig. 1B) or an irrelevant rabbit IgG (not shown). The specificity of the signal was confirmed by using the alternative anti-AChE ab31276 antibody (blot not shown). N-19 is a goat antiserum raised against a peptide that maps to the N terminus of human AChE, whereas ab31276 recognizes the C-terminal residues 601 to 614 of human AChE. We have previously observed a similar pattern of AChE labeling with both antibodies (21).

To confirm this interaction, we tried conversely to coimmunoprecipitate PS1 using anti-AChE antibodies (Fig. 1C and D). Brain AChE was immunoprecipitated using the MA3-042 antibody. Immunoblotting with 98/1 antibody readily detected a 29-kDa band corresponding to PS1-NTF (Fig. 1C). Immunoblotting with 00/2 antibody, raised to the PS1 loop region (see Fig. 1A) (16) revealed a faint 45-kDa band corresponding to PS1 holoprotein, but no band resembling PS1 C-terminal fragment (PS1-CTF; ~20 kDa) (Fig. 1D), demonstrating that PS1-NTF but not PS1-loop region interacts with AChE. The ~32-kDa band detected by 00/2 antibody and found to be enriched in immunoprecipitates (Fig. 1D) may correspond to the PS1 caspase cleavage product (30, 38, 54), although the identity of this peptide remains to be determined (34, 77). Omission of the anti-AChE antibody failed to immunoprecipitate these bands (Fig. 1C and D).

We further analyzed the in vitro interaction between AChE and PS1-NTF by an affinity matrix consisting of neurotoxin Fas2 coupled to Sepharose. About 90% of the AChE activity was bound to the affinity gel. Immunoblotting with N-19 antibody confirmed the presence of 70- and 55-kDa AChE bands in the bound fraction (Fig. 1E). Moreover, Fas-2 pulled down PS1-NTF from human brain extracts (Fig. 1E).

Cellular colocalization of PS1 and AChE. We used immunocytochemistry to compare the distribution of PS1 and AChE in wild-type COS-7 cells. Immunofluorescence labeling indicated localization of PS1 to endoplasmic reticulum-Golgi apparatus compartments and at the plasma membrane (Fig. 2A), a finding consistent with previous reports by us and others (11, 26, 31). AChE staining appeared contiguous with that of PS1, being very intense in the perinuclear region and at the plasma membrane, and diffuse throughout the cytoplasm (Fig. 2B).

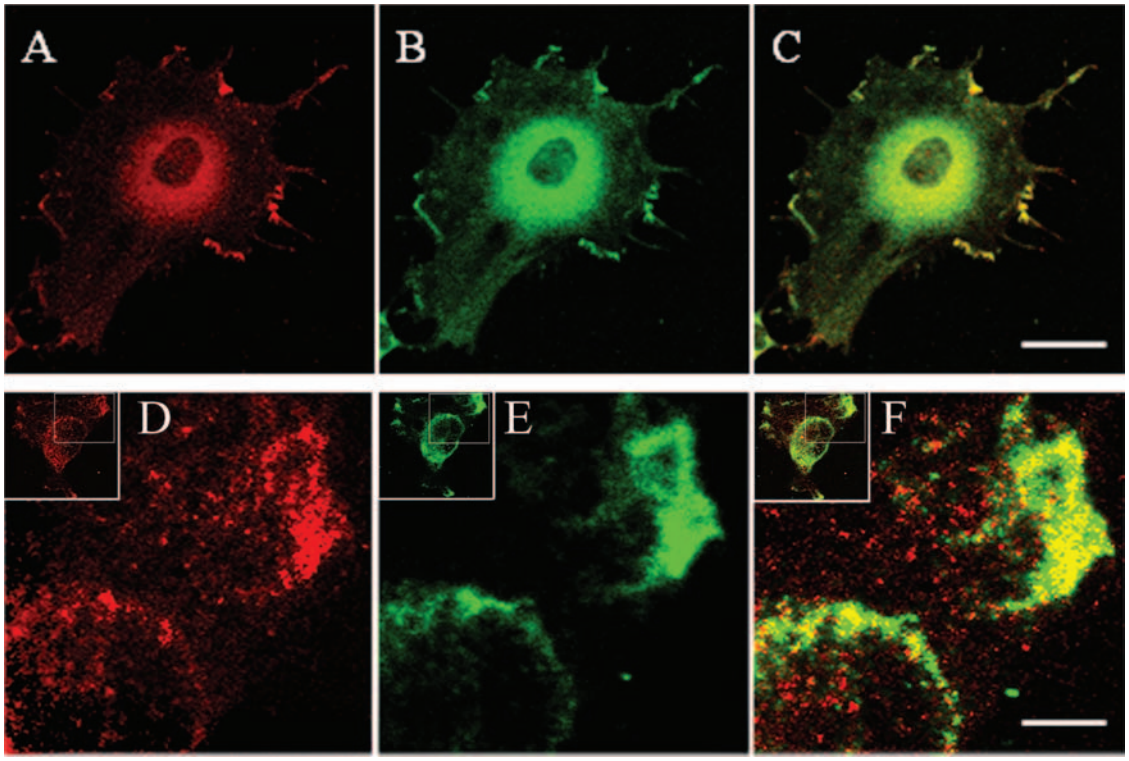

FIG. 2. Cellular colocalization of PS1 and AChE. (A and D) COS-7 cells were stained with the anti-PS1 antibody 98/1, followed by Alexa Fluor 555-labeled donkey anti-rabbit IgG (red). (B and E) The same cells were stained with the anti-AChE antibody MA3-042, followed by Alexa Fluor 488-labeled goat anti-mouse IgG (green). (C and F) Merged image showing colocalization (yellow). All images represent a single focal plane of the cell. (A to C) The images were obtained with a ×40 oil immersion objective lens (HCX PL, APO ×40, 1.25 oil). Scale bar, 50 μm. (D to F) Low-power (insets) and high-power pictures, showing the perinuclear and plasmatic membrane colocalization of PS1 with AChE, were taken with a ×63 oil immersion objective lens (HCX PL, APO ×63, 1.32 oil BD; single image section, 285.8 nm). Scale bar, 5 μm.

Control staining using secondary antibodies alone was negative (data not shown). Colocalization by merging images was evident in both the perinuclear region and the plasma membrane (Fig. 2C). This subcellular colocalization demonstrated with untransfected cells indicates that a possible in vivo interaction between PS1 and AChE can occur not only at the plasma membrane but also in the early compartments of the biosynthetic pathway.

Immunohistochemistry of PS1 and AChE in control and AD cortex. Histological examination of human frontal cortex was performed to confirm whether endogenous tissue PS1 and AChE are localized in the same intracellular compartments. The subcellular localization of PS1 and AChE was studied in the frontal cortices from two nonpathological, three sporadic AD, and four FAD-PS1-linked mutations (two U89L, one M139T, and one E318G) stained first with the PS1-NTF antibody and developed with carbiozamine solution (57); after photography and washing, the slides were then stained with anti-AChE antibody MA3-042 and developed by classical DAB–Tris-HCl solution, and the same fields were imaged (Fig. 3). Sections from control brain showed only weak immunoreactivity to both antibodies (Fig. 3A and B). As reported previously (14, 26, 40), in the AD frontal cortex PS1 is expressed prominently in the neurons of all AD brains, sporadic and familial. Importantly, immunocytochemical analysis confirmed that PS1 and AChE displayed a very similar subcellular staining in the perinuclear cytoplasm of cortical neurons (Fig. 3C to J). Immunopositive deposits were heterogeneously granular and distributed around the central nuclear area without specific segregation in relation to the cellular polarity. As previously documented (31, 37, 40), mutations of PS1 that cause FAD are not associated with changes in the subcellular localization of PS1. Hence, PS1 and AChE deposits colocalized in the same cytoplasmic regions of cortical neurons of FAD cases (inset in Fig. 3H).

Interaction of PS1 with AChE molecular forms differs in control and AD cortices. We aimed to determine whether PS1-AChE interaction was altered in the AD brain. As reported previously (18, 66), frontal cortex AChE activity was found to be decreased in sporadic AD (45%; $P = 0.02$) and to a greater extend (62% decrease; $P = 0.03$) in patients with FAD-PS1 linked mutations (two U89L, one M139T, and one E318G) compared to NDC (Fig. 4A). Despite differences in the banding pattern of AChE subunits between developmental and adult state, Western blotting analysis of adult brain PS1 immunoprecipitates with anti-AChE antibody demonstrated that a 55-kDa protein band was again the major AChE subunit coprecipitated with PS1 in both NDC and sporadic AD extracts (Fig. 4B). The percentage of AChE activity coimmunoprecipitated with PS1 (98/1 antibody) was similar for NDC and sporadic AD cases, and it was comparable to that in embryonic

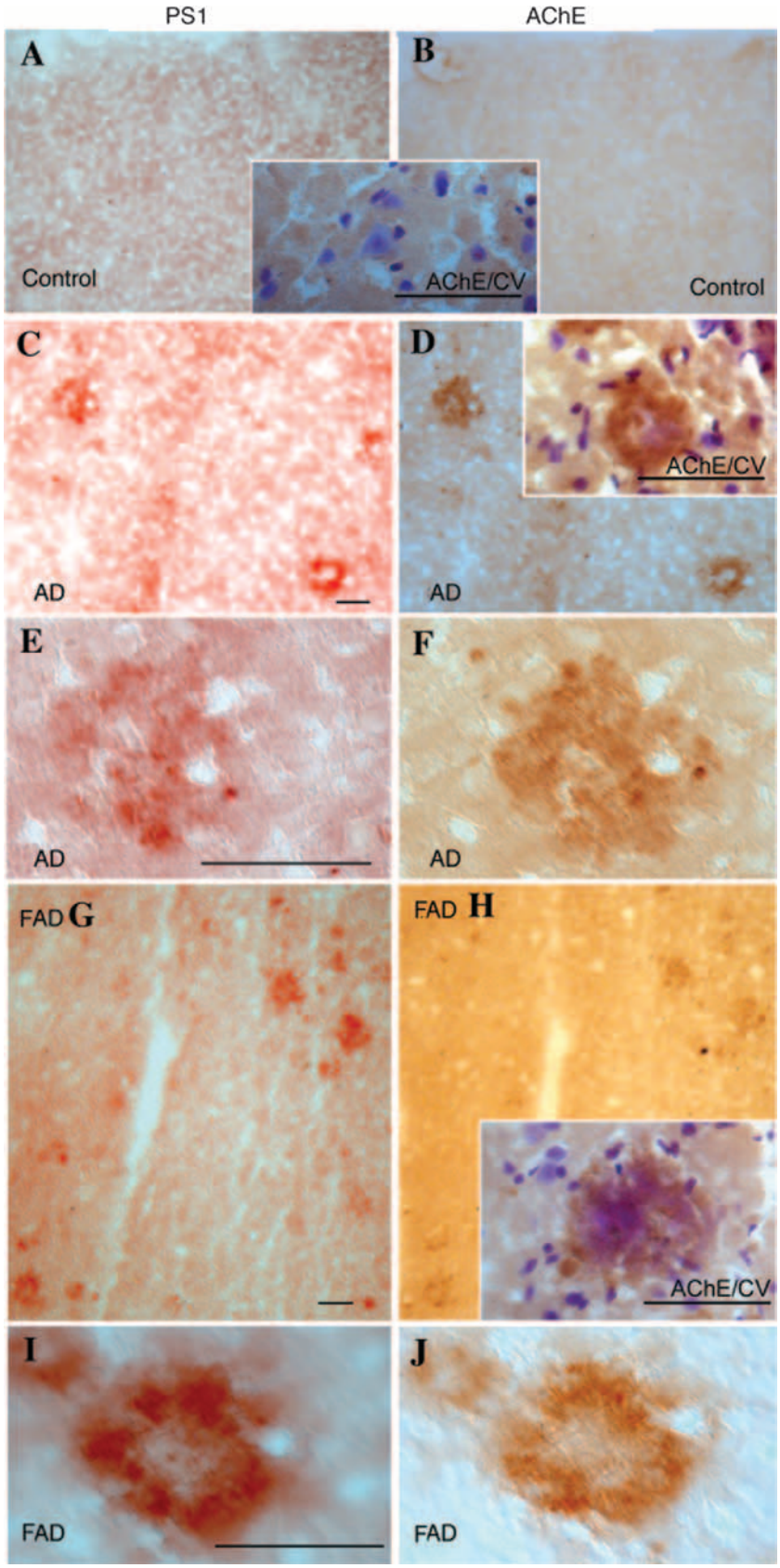

FIG. 3. Immunohistochemical detection of PS1 and AChE in human frontal cortex. Photographs of control cortex processed by anti-PS1 (A) or anti-AChE (B) antibody. The inset shows the section shown in panel B after cresyl violet (CV) staining. (C to F) Pictures from the

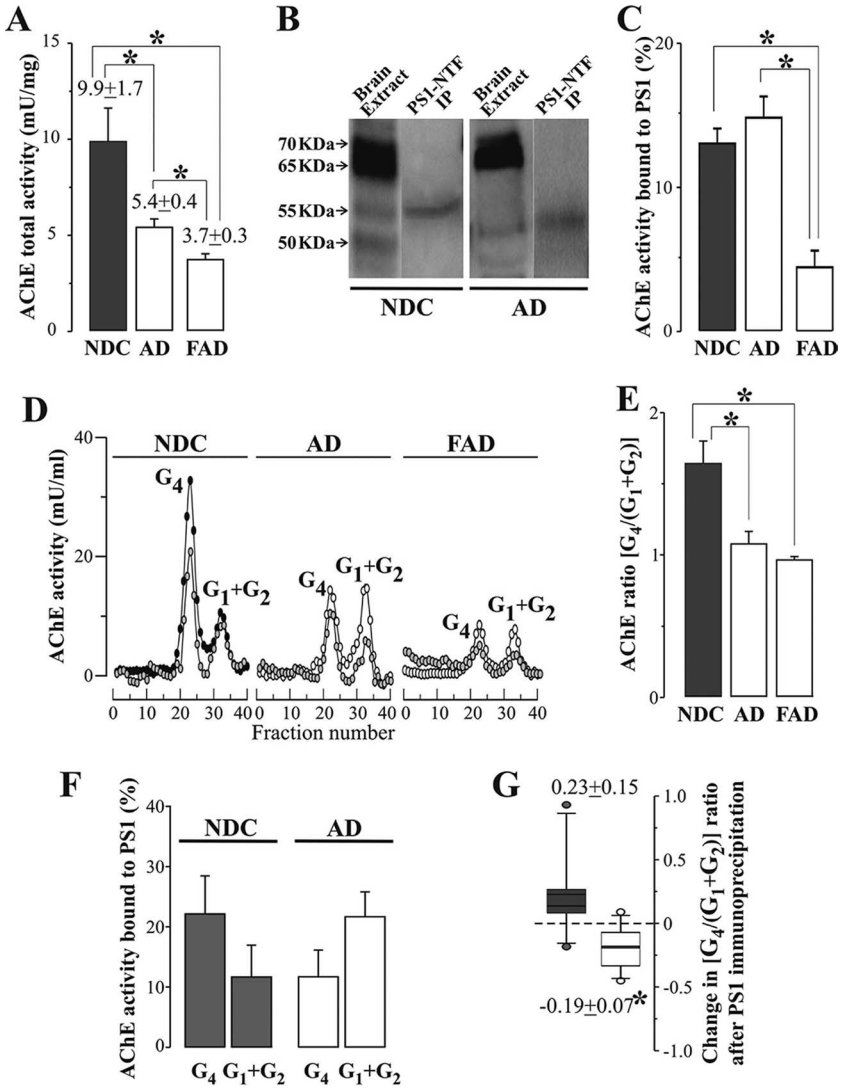

FIG. 4. Study of PS1-AChE interaction in human brain cortex samples from nonpathological and AD subjects. (A) Frontal cortex extracts from NDC, sporadic AD patients (AD), and FAD mutation cases (two cases bearing the V89L mutation, one bearing the M139T mutation, and one bearing the E318G mutation; see Materials and Methods for details) were assayed for total AChE activity. (B) Immunoprecipitation of brain extracts with anti-PS1 antibody, 98/1, followed by immunoblotting with anti-AChE antibody, N-19. (C) Averaged percentage of AChE activity coimmunoprecipitated for each subgroup. (D and E) Representative profiles of AChE molecular forms (D) and the $G_4/(G_2+G_1)$ molecular ratio for each group (E). The data represent the means ± the standard error of the mean (determinations in triplicate). The data were analyzed by using one-way analysis of variance with the Bonferroni posttest to compare all groups, and exact *P* values were determined by using the Student *t* test. *, $P < 0.05$. (F and G) Percentage of AChE molecular forms coprecipitated with PS1 for control (NDC) and sporadic AD (AD) cases (F) and change in the $G_4/(G_2+G_1)$ ratio before and after PS1 immunoprecipitation (G). *, significantly different ($P < 0.05$) from the NDC group.

tissue, whereas we found decreased coimmunoprecipitation in PS1-FAD subjects (Fig. 4C).

AChE exhibits complex structural polymorphism (39) with a molecular form pattern which is altered in AD (18, 66, 70). Accordingly, we found that the major G_4 peak decreased in AD frontal cortex extracts, with minimal change in minor G_2 and G_1 species, resulting in a decrease ($P \leq 0.01$) in the ratio of AChE molecular forms in sporadic AD [$G_4/(G_1+G_2) = 1.08 \pm 0.09$] and FAD [$G_4/(G_1+G_2) = 0.96 \pm 0.02$] compared to NDC [$G_4/(G_1+G_2) = 1.64 \pm 0.16$] (Fig. 4D and E). Given

same cortical section of a sporadic AD patient. Deposits of PS1 (C and E) and AChE (D and F) were colocalized in the cerebral cortex. The inset in panel D shows how the deposits are localized in the perinuclear region of the cytoplasm when the cellular staining by cresyl violet was still detectable. (G to J) Photographs showing the same cortical section of a FAD patient (FAD). PS1 (G and I) and AChE (H and J) deposits colocalized in the same regions of the cortex. These deposits corresponded to perinuclear areas in the cytoplasm of large cortical cells (inset in panel H). Scale bars, 100 μm.

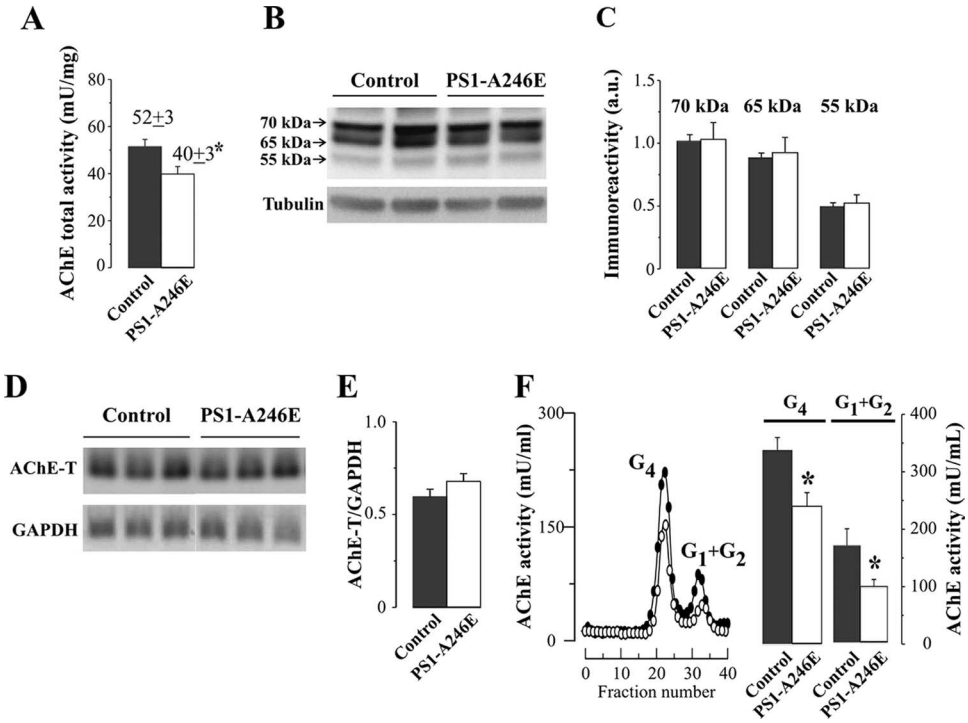

FIG. 5. Mutant PS1-A246E alters AChE activity levels. (A and B) Cortical AChE activity (A) and immunodetection of brain AChE variants with the antibody E-19 from PS1-A246E and control mice (equivalent amounts of protein were loaded in each lane) (B). (C) Densitometric quantification of the major AChE immunopositive bands. The results were normalized by using the tubulin immunoreactivity for each sample (no comparisons were statistically significant). (D) Detection of AChE-T transcripts by semiquantitative RT-PCR using selected primers (1bs [in the common exon 3], 5′-TCAGCGACTTATGAAATACTGGA-3′; Ta [in the "tailed" T region, also called exon 6], 5′TTCCAGTGCACCATGT AGGA 3′) and the products identified according to their sizes. (E) Graphic representation of the AChE-T mRNA levels relative to GAPDH. (F) Representative profiles and levels of molecular AChE forms in the cortex extracts of 9-month-old PS1-A246E mice ($n = 7$) and age-matched nontransgenic controls ($n = 7$). *, Significantly different ($P < 0.05$) from control mice.

that the proportions of AChE species varied in the AD brain, we investigated whether PS1 preferentially interacts with a specific molecular form of AChE. For this purpose, AChE forms were separated and quantified for enzymatic activity in the unbound fraction after PS1 immunoprecipitation. In the NDC supernatants we determined that PS1 preferentially coprecipitates G_4 compared to G_1+G_2 species, whereas in sporadic AD AChE light species displayed higher affinity for PS1 than for the G_4 form (Fig. 4F). Consequently, sporadic AD and NDC statistically differed ($P = 0.02$) in their AChE [$G_4/(G_1+G_2)$] molecular ratios before and after PS1 immunoprecipitation (Fig. 4G).

AChE levels and glycosylation are altered in PS1 A246E transgenic mouse brain. Mutations in PS1 trigger the earliest age of onset and the most aggressive forms of AD. By causing a loss of γ-secretase function these mutations affect APP processing and Aβ production (79), but they may also affect processing and trafficking of other substrates and interacting proteins since presenilins are implicated in many cellular functions (reviewed in reference 51). To determine whether a pathogenic PS1 mutation may influence AChE expression, we examined AChE levels in brains of 9-month-old transgenic mice expressing human PS1-A246E mutation (58). We confirmed that at this age, the brains of PS1-A246E mice were free of any AD-like pathology. Assay of AChE revealed that cortical extracts from PS1-A246E mice had lower activity (22% decrease; $P = 0.02$) compared to those of nontransgenic controls (Fig. 5A). Because AChE occurs as both active and inactive subunits (8, 64), we also examined AChE protein levels by immunoblotting to assess whether overexpression of mutant PS1 can affect maturation/processing of AChE. We analyzed mouse cortical extracts by SDS-PAGE under fully reducing conditions, followed by Western blotting with the anti-AChE antibody E-19. This polyclonal antibody was raised against a peptide mapping to the amino terminus of AChE, common to all AChE forms and thus presumably detects all species, including inactive subunits (21). E-19 detected three major bands of approximately 70, 60, and 55 kDa (Fig. 5B). Neither the intensity of the individual bands nor their relative banding pattern was altered in transgenic mice compared to controls (Fig. 5C). We interpret the lack of correlation between decreased brain cortical AChE activity and unaltered immunoreactivity to mean that the total pool of AChE protein, containing active and inactive (noncatalytic) subunits, remains unaltered in the transgenic mouse brain. To determine whether AChE expression is altered in the transgenic mice, we performed semiquantitative RT-PCR analysis of the AChE mRNA. The levels of the T-transcript, the major transcript in mammal brain (52), was unaltered in cortices from PS1-A246E transgenic mice compared to controls (Fig. 5D and E). We did not detect noticeable R-transcript, an alternatively spliced

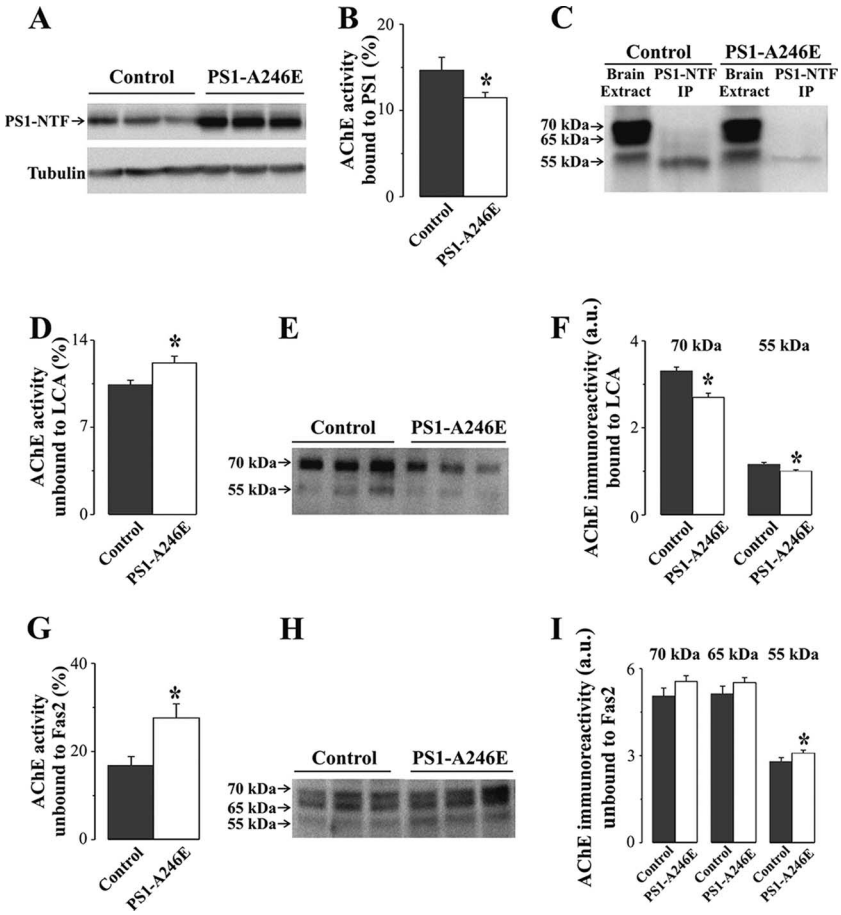

FIG. 6. Effect of mutant PS1-A246E on PS1-AChE interaction and on AChE glycosylation and accessibility to its peripheral binding site. (A) Concentrations and gel mobility analysis of PS1-NTF in PS1-A246E and control mouse brain. (B) Percentage of AChE coimmunoprecipitated with the anti-PS1 antibody 98/1. (C) Immunoblotting analysis of 98/1-precipitated proteins with the anti-AChE antibody E-19. (D) Comparison of LCA binding of AChE from PS1-A246E and control mice. Cortex extracts of 9-month-old PS1-A246E mice ($n = 7$) and age-matched nontransgenic controls ($n = 7$) were incubated with immobilized LCA, and the percentage of AChE activity unbound to the lectin was calculated. (E) Western blot analysis of the lectin-bound fraction with antibody E-19. (F) Densitometric quantification of the AChE-immunoreactive bands binding to LCA. (G) Comparison of Fas2 binding of AChE from PS1-A246E and control mice. Cortex extracts were incubated with immobilized Fas2, and the percentage of AChE activity unbound was calculated. (H) Western blot analysis of AChE-banding pattern of the unbound fraction. (I) Densitometric quantification of the AChE-immunoreactive bands was performed. *, significantly different ($P < 0.05$) from control mice.

AChE transcript that is scarce in mammal brain and seems to be induced under stress (29, 52).

To determine whether the observed decrease in AChE activity was due to a decrease of a particular molecular form of the enzyme, brain cortical supernatants were fractionated on sucrose density gradients to separate AChE species (Fig. 5F). In the PS1-A246E transgenic cortices, both peaks corresponding to the major AChE tetramers (G_4) and to the minor light forms (dimers [G_2] and monomers [G_1]) were decreased similarly. Consequently, the ratio of AChE molecular forms, $G_4/(G_1+G_2)$, did not vary compared to controls (not shown).

The PS1-A246E mutation resides in PS1 NTF (see Fig. 1A) and does not conspicuously alter proteolytic processing of the PS1 variant in brain (3). Consequently, we found increased amounts of PS1 NTF in the brains of transgenic mice compared to control wild-type mice (Fig. 6A). Nevertheless, the proportion of AChE that coimmunoprecipitated with PS1 was decreased in the PS1-A246E transgenic mice, compared to the controls (Fig. 6B). Once again, a 55-kDa band was the predominant AChE subunit in PS1 immunoprecipitates (Fig. 6C).

Our results and the increased experimental evidence that PS1 has a role in the trafficking, maturation, and stabilization of other glycoproteins than APP and γ-secretase components (24, 45) led us to further investigate whether the PS1-A246E mutation causes impaired glycosylation of AChE. First, to compare the pattern of AChE glycosylation in transgenic and nontransgenic mice, equivalent amounts of protein from cortical extracts were incubated with immobilized lectins, proteins that avidly bind to specific sugar moieties of glycoproteins. There was a small but significant ($P = 0.02$) increase in the percentage of AChE activity unbound to LCA, a plant lectin that recognizes sequences containing terminal α-linked mannose residues (67) in the PS1-A246E compared to controls (Fig. 6D). In accordance, Western blot analysis of the LCA bound-protein fraction confirmed decreased AChE immunoreactivity for the 70-kDa ($P = 0.002$) and 55-kDa ($P = 0.001$) bands in PS1-A246E extracts (Fig. 6E and F).

We further investigated changes in AChE protein properties by incubation with Fas2-Sepharose, which binds to the peripheral anionic site (PAS) of the enzyme (4). This site is involved in AChE catalytic activity and in heterologous protein associations, including nucleation of amyloid peptides (27). There was reduced binding of AChE to Fas2 ($P = 0.03$) in cortical extracts of PS1-A246E compared to controls (Fig. 6G), suggesting a structural difference between control and mutant mouse AChE. Western blot analysis of the unbound fraction identified the 55-kDa band as the AChE subunit with decreased capacity to bind Fas2 ($P = 0.03$) (Fig. 6H and I).

DISCUSSION

There has been an extensive effort to identify proteins that functionally interact with PS1 because of their possible implications in AD. We present evidence here that PS1 can physically interact with AChE in human brain. Coimmunoprecipitation of AChE with PS1 was observed in both embryonic and adult brain homogenates. Reciprocal coimmunoprecipitation and affinity-binding coprecipitation confirmed this interaction and the involvement of PS1-NTF. Accordingly, the PS1-A246E mutation, which resides in the C-terminal portion of the NTF of PS1, markedly reduced the efficiency of the PS1-AChE interaction. However, the human brain samples analyzed, including other FAD-PS1 mutations in the CTF, also exhibit decreased affinity for AChE. Thus, we cannot rule out that NTF-CTF interactions, which present a subcellular codistribution and a 1:1 stoichiometric relationship (2, 77), can also modulate the PS1-AChE interaction.

The adhesion-promoting PAS region of AChE have been is involved in the promotion of Aβ fibril formation (27). We found that the binding of AChE to neurotoxin Fas2, a potent allosteric AChE inhibitor that occupies the PAS of the enzyme, did not prevent the binding of AChE to PS1. Thus, the tethering of PS1 to Fas2-bound AChE indicated that the interaction of PS1 with AChE does not depend on the adhesive functions attributed to the PAS.

We observed that ~15% of human and mouse brain AChE activity pulled down with the anti-PS1 antibody mostly migrated as a 55-kDa band. This would correspond to the 55-kDa subunit that is contained within both AChE tetramers and monomers species (20, 21); thus, it cannot be assigned to a particular AChE form. Accordingly, PS1 may coprecipitate either the G_4 or the G_1+G_2 species or both of them. Using nondenaturing polyacrylamide gels stained for AChE activity, the molecular masses of AChE subunits are in the range of 70 to 75 kDa. Analysis by SDS-PAGE and Western blotting by us and others, under fully reducing conditions and with several alternative anti-AChE antibodies, detected bands ranging from 75 to 60 kDa, as well as other species of 55 and 50 kDa, that may have originated by posttranslation modification (12, 20, 21, 74). In a previous study, we confirmed the specificity of the major AChE bands, including the 55-kDa subunit, by AChE immunoprecipitation and probing blots with three alternative anti-human AChE antibodies (21). Fas2 affinity matrix also pulled down the 55-kDa AChE band. The identity of a 55-kDa AChE species as an AChE-specific protein has been confirmed in another recent study by competitive assays, AChE immunoprecipitation, and mass spectrometry (68). Moreover, we cannot discount that the PS1-AChE interaction may involve some immature/inactive AChE species, but the finding of a reduction of AChE activity after coprecipitation with PS1 indicates that the interaction does involve some active AChE. The limited extent of the endogenous interaction may be related to the multiple interaction partners of PS1 in the cell.

Confocal microscopy analysis in COS-7 cells not only confirms the subcellular localization of PS1 but also documents that PS1 and AChE have intracellular overlapping distributions through the endoplasmic reticulum-Golgi apparatus, suggesting that PS1 may regulate the maturation and trafficking of AChE in early compartments of the biosynthetic pathway. Immunohistochemical study of the human frontal cortex supports the view that PS1 and AChE are localized in same intracellular compartments. Although the evidence implying that PS1 is involved in the processing of APP, Notch, and other substrates is strong, it remains an issue of debate whether PS1 has a more general role in the trafficking, maturation, and stabilization of different proteins (9, 45). Thus, the role of PS1 in trafficking can be distinguished from γ-secretase activity. Previous studies showed that the bulk of endogenously expressed PS1 in neurons is located in the early compartments of the biosynthetic pathway (2, 11, 26, 31). These findings are consistent with roles for PS1 in facilitating the processing and intracellular trafficking of proteins undergoing posttranslational modification.

PS1 has been implicated in the physiological maturation and glycosylation of APP (28, 35, 45) and other glycoproteins such as nicastrin (36, 72), BACE1 (24), and TrkB (45). It has been suggested that overexpression of PS1 disturbs glycosylation processing within the Golgi apparatus (17). All of these observations suggest that PS1 may be implicated in the glycosylation and/or maturation of a selected set of membrane and secretory proteins in neurons, possibly including AChE. In this context, we found that the transgenic mice expressing FAD-linked A246 human PS1 variant showed altered AChE glycosylation.

It has been established that protein conformation and function can seriously be compromised by abnormal incorporation of carbohydrate moieties in glycoproteins. The expression of the PS1-A246E transgene decreases brain AChE activity without affecting total AChE protein content. The changed accessibility in mutant mice of Fas2 to the PAS of AChE, which is also involved in its catalytic activity, may reflect a shift in protein conformation. The altered ratio of active to inactive AChE correlates with decreased affinity of PS1-A246E for AChE and provides evidence that in PS1 mutant mice the maturation of catalytic subunits of AChE is impaired, and therefore less-mature active species of AChE are present in these animals. We hypothesize that PS1 is implicated in posttranslational processing, including correct glycosylation of AChE; thus, a loss of function of PS1 caused by the FAD mutation may disturb AChE maturation.

Correct glycosylation also determines the adequate intracellular trafficking, folding, assembly, and final localization of glycoproteins, playing a vital role in biological processes such as protein-protein interactions. In previous reports (65, 66), we showed that AD brain contains abnormally glycosylated AChE. This change in glycosylation was specific for a minor subset of G_1 AChE, whose contribution increased in the AD brain (66). Therefore, conversely altered AChE glycosylation

may be related to the detected switch in affinity of PS1 for AChE molecular species in AD brain extracts.

Likewise, the FAD-linked A246E effect on AChE activity levels in the transgenic mice may have functional consequences. Although transgenic mice expressing A246E-PS1 do not develop neuritic plaques, they show defects in hippocampal long-term potentiation (50) and neurogenesis (10), as well as alteration of distinct motor responses (33). Multiple lines of evidence point to the participation and/or modulation of these processes by AChE (48, 62, 73, 81). Thus, AChE deficit in PS1-A246E transgenic mice may contribute to the described dysfunctions, similarly as cholinergic impairment contributes to cognitive and functional symptoms of AD.

The presence of AChE in association with amyloid has yet to be explained. Most cortical AChE activity present in the AD brain is associated with neuritic plaques (42, 78) and displays particular enzymatic properties and sensitivity to inhibitors (22, 80). It is unclear whether these changes contribute to the capacity to accelerate the assembly of β-amyloid (27) or, alternatively, whether they are the consequence of Aβ influence on AChE expression (25, 69).

Several authors have reported the involvement of cholinergic mechanisms in the regulation of amyloid metabolism (15, 49, 63). A role for PS1 in the regulation of muscarinic receptor-mediated signal transduction has also been suggested (55). Here, we show the cell surface colocalization of PS1 and AChE in COS-7 cells in addition to their predominant perinuclear colocalization. The possibility that both PS1 and AChE are targeted together to the plasma membrane of neuronal cells may have physiological consequences such as a fine-tuning of muscarinic responses and/or modulation of amyloid metabolism.

Finally, very few studies have analyzed whether PS1 influences AChE expression or vice versa. A recent report revealed altered levels of AChE activity in mutant PS2 transgenic brains from senescent animals compared to the wild-type PS2 transgenic and nontransgenic mice (46). Another study with transgenic mice overexpressing AChE indicated increased mRNA expression of PS1 in neuronal cells (61).

We have described here for the first time the molecular association between PS1 and AChE, which may be relevant to the pathological progress of dementia in AD and to the design of therapeutic strategies. The observation of an interaction between PS1 and AChE, together with its alteration in presence of PS1 FAD mutations, supports the notion of a cholinergic-amyloid interrelationship. Further study is needed to clarify the functional role of this interaction and whether the PS1 loss of function has an effect on AChE activity and vice versa, which could have important consequences since these two enzymes are therapeutic targets in AD.

ACKNOWLEDGMENTS

We thank M. Calero (Centro Nacional de Microbiologia, Instituto de Salud Carlos III, Majadahonda, Madrid, Spain) for helpful advice; S. Ramón y Cajal and N. Torán (Department of Pathology, Hospital Vall d'Hebron, Barcelona, Spain) for assistance with accessing human embryonic samples; and R. Bruno, R. Rivera, and M. Ródenas for technical assistance.

M.-X.S. is a fellow of CSIC (MEC) from Spain. G.E. and J.G.C. are supported by the Australian NHMRC. This study was supported by grants from the la Caixa Foundation, FIS (grants 03/0038 and 06/0181), and CIBERNED, ISC-III (Spain), to J.S.-V.

REFERENCES

1. **Aldudo, J., M. J. Bullido, A. Frank, and F. Valdivieso.** 1998. Missense mutation E318G of the presenilin-1 gene appears to be a nonpathogenic polymorphism. Ann. Neurol. **44:**985–986.
2. **Annaert, W. G., L. Levesque, K. Craessaerts, I. Dierinck, G. Snellings, and D. Westaway.** 1999. Presenilin 1 controls γ-secretase processing of amyloid precursor protein in pre-Golgi compartments of hippocampal neurons. J. Cell Biol. **147:**277–294.
3. **Borchelt, D. R., G. Thinakaran, C. B. Eckman, M. K. Lee, F. Davenport, T. Ratovitsky, C. M. Prada, G. Kim, S. Seekins, D. Yager, H. H. Slunt, R. Wang, M. Seeger, A. I. Levey, S. E. Gandy, N. G. Copeland, N. A. Jenkins, D. L. Price, S. G. Younkin, and S. S. Sisodia.** 1996. Familial Alzheimer's disease-linked presenilin 1 variants elevate Aβ1-42/1-40 ratio in vitro and in vivo. Neuron **17:**1005–1013.
4. **Bourne, Y., P. Taylor, Z. Radic, and P. Marchot.** 2003. Structural insights into ligand interactions at the acetylcholinesterase peripheral anionic site. EMBO J. **22:**1–12.
5. **Braak, H., and E. Braak.** 1998. Evolution of neuronal changes in the course of Alzheimer's disease. J. Neural Transm. Suppl. **53:**127–140.
6. **Campion, D., J. M. Flaman, A. Brice, D. Hannequin, B. Dubois, C. Martin, V. Moreau, F. Charbonnier, O. Didierjean, S. Tardieu, C. Penet, M. Puel, F. Pasquier, F. Le Doze, G. Bellis, A. Calenda, R. Heilig, M. Martinez, J. Mallet, M. Bellis, F. Clerget-Darpoux, Y. Agid, and T. Frebourg.** 1995. Mutations of the presenilin I gene in families with early-onset Alzheimer's disease. Hum. Mol. Genet. **4:**2373–2377.
7. **Capell, A., J. Grünberg, B. Pesold, A. Diehlmann, M. Citron, R. Nixon, K. Beyreuther, D. J. Selkoe, and C. Haass.** 1998. The proteolytic fragments of the Alzheimer's disease-associated presenilin-1 form heterodimers and occur as a 100-150-kDa molecular mass complex. J. Biol. Chem. **273:**3205–3211.
8. **Chatel, J. M., J. Grassi, Y. Frobert, J. Massoulié, and F. M. Vallette.** 1993. Existence of an inactive pool of acetylcholinesterase in chicken brain. Proc. Natl. Acad. Sci. USA **90:**2476–2480.
9. **Chen, F., D. S. Yang, S. Petanceska, A. Yang, A. Tandon, G. Yu, R. Rozmahel, J. Ghiso, M. Nishimura, D. M. Zhang, T. Kawarai, G. Levesque, J. Mills, L. Levesque, Y. Q. Song, E. Rogaeva, D. Westaway, H. Mount, S. Gandy, P. St George-Hyslop, and P. E. Fraser.** 2000. Carboxyl-terminal fragments of Alzheimer beta-amyloid precursor protein accumulate in restricted and unpredicted intracellular compartments in presenilin 1-deficient cells. J. Biol. Chem. **275:**36794–36802.
10. **Chevallier, N. L., S. Soriano, D. E. Kang, E. Masliah, G. Hu, and E. H. Koo.** 2005. Perturbed neurogenesis in the adult hippocampus associated with presenilin-1 A246E mutation. Am. J. Pathol. **167:**151–159.
11. **Culvenor, J. G., F. Maher, G. Evin, F. Malchiodi-Albedi, R. Cappai, J. R. Underwood, J. B. Davis, E. H. Karran, G. W. Roberts, K. Beyreuther, and C. L. Masters.** 1997. Alzheimer's disease-associated presenilin 1 in neuronal cells: evidence for localization to the endoplasmic reticulum-Golgi intermediate compartment. J. Neurosci. Res. **49:**719–731.
12. **Darreh-Shori, T., E. Hellstrom-Lindahl, C. Flores-Flores, Z. Z. Guan, H. Soreq, and A. Nordberg.** 2004. Long-lasting acetylcholinesterase splice variations in anticholinesterase-treated Alzheimer's disease patients. J. Neurochem. **88:**1102–1113.
13. **Davies, P., and A. J. Maloney.** 1976. Selective loss of central cholinergic neurons in Alzheimer's disease. Lancet **i:**1403.
14. **Diehlmann, A., N. Ida, S. Weggen, J. Grunberg, C. Haass, C. L. Masters, T. A. Bayer, and K. Beyreuther.** 1999. Analysis of presenilin 1 and presenilin 2 expression and processing by newly developed monoclonal antibodies. J. Neurosci. Res. **56:**405–419.
15. **Efthimiopoulos, S., D. Vassilacopoulou, J. A. Ripellino, N. Tezapsidis, and N. K. Robakis.** 1996. Cholinergic agonists stimulate secretion of soluble full-length amyloid precursor protein in neuroendocrine cells. Proc. Natl. Acad. Sci. USA **93:**8046–8050.
16. **Evin, G., R. A. Sharples, A. Weidemann, F. B. Reinhard, V. Carbone, J. G. Culvenor, R. M. Holsinger, M. F. Sernee, K. Beyreuther, and C. L. Masters.** 2001. Aspartyl protease inhibitor pepstatin binds to the presenilins of Alzheimer's disease. Biochemistry **40:**8359–8368.
17. **Farquhar, M. J., C. W. Gray, and K. C. Breen.** 2003. The overexpression of the wild-type or mutant forms of the presenilin-1 protein alters glycoprotein processing in a human neuroblastoma cell line. Neurosci. Lett. **346:**53–56.
18. **Fishman, E. B., G. C. Siek, R. D. MacCallum, E. D. Bird, L. Volicer, and J. K. Marquis.** 1986. Distribution of the molecular forms of acetylcholinesterase in human brain: alterations in dementia of the Alzheimer type. Ann. Neurol. **19:**246–252.
19. **Gandy, S. J.** 2005. The role of cerebral amyloid beta accumulation in common forms of Alzheimer disease. J. Clin. Investig. **115:**1121–1129.
20. **García-Ayllón, M. S., M. X. Silveyra, A. Candela, A. Compañ, J. Clària, R. Jover, M. Pérez-Mateo, V. Felipo, S. Martínez, J. Galcerán, and J. Sáez-Valero.** 2006. Changes in liver and plasma acetylcholinesterase in rats with cirrhosis induced by bile duct ligation. Hepatology **43:**444–453.

21. **García-Ayllón, M. S., M. X. Silveyra, N. Andreasen, S. Brimijoin, K. Blennow, and J. Sáez-Valero.** 2007. Cerebrospinal fluid acetylcholinesterase changes after treatment with donepezil in patients with Alzheimer's disease. J. Neurochem. **101:**1701–1711.
22. **Geula, C., and M. Mesulam.** 1989. Special properties of cholinesterases in the cerebral cortex of Alzheimer's disease. Brain Res. **498:**185–189.
23. **Hashimoto, Y., E. Tsukamoto, T. Niikura, Y. Yamagishi, M. Ishizaka, S. Aiso, A. Takashima, and I. Nishimoto.** 2004. Amino- and carboxyl-terminal mutants of presenilin 1 cause neuronal cell death through distinct toxic mechanisms: study of 27 different presenilin 1 mutants. J. Neurosci. Res. **75:**417–428.
24. **Hébert, S. S., V. Bourdages, C. Godin, M. Ferland, M. Carreau, and G. Lévesque.** 2003. Presenilin-1 interacts directly with the beta-site amyloid protein precursor cleaving enzyme (BACE1). Neurobiol. Dis. **13:**238–245.
25. **Hu, W., N. W. Gray, and S. Brimijoin.** 2003. Amyloid-beta increases acetylcholinesterase expression in neuroblastoma cells by reducing enzyme degradation. J. Neurochem. **86:**470–478.
26. **Huynh, D. P., H. V. Vinters, D. H. Ho, V. V. Ho, and S. M. Pulst.** 1997. Neuronal expression and intracellular localization of presenilins in normal and Alzheimer disease brains. J. Neuropathol. Exp. Neurol. **56:**1009–1017.
27. **Inestrosa, N. C., A. Alvarez, C. A. Pérez, R. D. Moreno, M. Vicente, C. Linker, O. I. Casanueva, C. Soto, and J. Garrido.** 1996. Acetylcholinestearse accelerates assembly of amyloid-beta-peptides into Alzheimer's fibrils: possible role of the peripheral site of the enzyme. Neuron **16:**881–891.
28. **Kaether, C., S. Lammich, D. Edbauer, M. Ertl, J. Rietdorf, A. Capell, H. Steiner, and C. Haass.** 2002. Presenilin-1 affects trafficking and processing of βAPP and is targeted in a complex with nicastrin to the plasma membrane. J. Cell Biol. **158:**551–561.
29. **Kaufer, D., A. Friedman, S. Seidman, and H. Soreq.** 1998. Acute stress facilitates long-lasting changes in cholinergic gene expression. Nature **393:** 373–377.
30. **Kim, T. W., W. H. Pettingell, Y. K. Jung, D. M. Kovacs, and R. E. Tanzi.** 1997. Alternative cleavage of Alzheimer-associated presenilins during apoptosis by a caspase-3 family protease. Science **277:**373–376.
31. **Kovacs, D. M., H. J. Fausett, K. J. Page, T. W. Kim, R. D. Moir, D. E. Merriam, R. D. Hollister, O. G. Hallmark, R. Mancini, K. M. Felsenstein, B. T. Hyman, R. E. Tanzi, and W. Wasco.** 1996. Alzheimer-associated presenilins 1 and 2: neuronal expression in brain and localization to intracellular membranes in mammalian cells. Nat. Med. **2:**224–229.
32. **Lahiri, D. K., S. Lewis, and M. R. Farlow.** 1994. Tacrine alters the secretion of the beta-amyloid precursor protein in cell lines. J. Neurosci. Res. **37:**777–787.
33. **Lalonde, R., S. Qian, and C. Strazielle.** 2003. Transgenic mice expressing the PS1-A246E mutation: effects on spatial learning, exploration, anxiety, and motor coordination. Behav. Brain Res. **138:**71–79.
34. **Lee, M. K., H. H. Slunt, L. J. Martin, G. Thinakaran, G. Kim, S. E. Gandy, M. Seeger, E. Koo, D. L. Price, and S. S. Sisodia.** 1996. Expression of presenilin 1 and 2 (PS1 and PS2) in human and murine tissues. J. Neurosci. **16:**7513–7525.
35. **Leem, J. Y., C. A. Saura, C. Pietrzik, J. Christianson, C. Wanamaker, L. T. King, M. L. Veselits, T. Tomita, L. Gasparini, T. Iwatsubo, H. Xu, W. N. Green, E. H. Koo, and G. Thinakaran.** 2002. A role for presenilin 1 in regulating the delivery of amyloid precursor protein to the cell surface. Neurobiol. Dis. **11:**64–82.
36. **Leem, J. Y., S. Vijayan, P. Han, D. Cai, M. Machura, K. O. Lopes, M. L. Veselits, H. Xu, and G. Thinakaran.** 2002. Presenilin 1 is required for maturation and cell surface accumulation of nicastrin. J. Biol. Chem. **277:** 19236–19240.
37. **Levey, A. I., C. J. Heilman, J. J. Lah, N. R. Nash, H. D. Rees, M. Wakai, S. S. Mirra, D. B. Rye, D. Nochlin, T. D. Bird, and E. J. Mufson.** 1997. Presenilin-1 protein expression in familial and sporadic Alzheimer's disease. Ann. Neurol. **41:**742–753.
38. **Loetscher, H., U. Deuschle, M. Brockhaus, D. Reinhardt, P. Nelboeck, J. Mous, J. Grünberg, C. Haass, and H. Jacobsen.** 1997. Presenilins are processed by caspase-type proteases. J. Biol. Chem. **272:**20655–20659.
39. **Massoulié, J.** 2002. The origin of the molecular diversity and functional anchoring of cholinesterases. Neurosignals **11:**130–143.
40. **Mathews, P. M., A. M. Cataldo, B. H. Kao, A. G. Rudnicki, X. Qin, J. L. Yang, Y. Jiang, M. Picciano, C. Hulette, C. F. Lippa, T. D. Bird, D. Nochlin, J. Walter, C. Haass, L. Lévesque, P. E. Fraser, A. Andreadis, and R. A. Nixon.** 2000. Brain expression of presenilins in sporadic and early-onset, familial Alzheimer's disease. Mol. Med. **6:**878–891.
41. **Mattila, K. M., C. Forsell, T. Pirttilä, J. O. Rinne, T. Lehtimäki, M. Röyttä, L. Lilius, A. Eerola, P. H. St George-Hyslop, H. Frey, and L. Lannfelt.** 1998. The Glu318Gly mutation of the presenilin-1 gene does not necessarily cause Alzheimer's disease. Ann. Neurol. **44:**965–967.
42. **Morán, M. A., E. J. Mufson, and P. Gómez-Ramos.** 1994. Cholinesterases colocalize with sites of neurofibrillary degeneration in aged and Alzheimer's brains. Acta Neuropathol. **87:**284–292.
43. **Mori, F., C. C. Lai, F. Fusi, and E. Giacobini.** 1995. Cholinesterase inhibitors increase secretion of APPs in rat brain cortex. Neuroreport **6:**633–636.
44. **Murayama, O., T. Tomita, N. Nihonmatsu, M. Murayama, X. Sun, T. Honda, T. Iwatsubo, and A. Takashima.** 1999. Enhancement of amyloid beta 42 secretion by 28 different presenilin 1 mutations of familial Alzheimer's disease. Neurosci. Lett. **265:**61–63.
45. **Naruse, S., G. Thinakaran, J. J. Luo, J. W. Kusiak, T. Tomita, T. Iwatsubo, X. Qian, D. D. Ginty, D. L. Price, D. R. Borchelt, P. C. Wong, and S. S. Sisodia.** 1998. Effects of PS1 deficiency on membrane protein trafficking in neurons. Neuron **21:**1213–1221.
46. **Nguyen, H. N., D. Y. Hwang, Y. K. Kim, D. Y. Yoon, J. H. Kim, M. S. Lee, M. K. Lee, Y. P. Yun, K. W. Oh, and J. T. Hong.** 2005. Mutant presenilin 2 increases acetylcholinesterase activity in neuronal cells. Arch. Pharm. Res. **28:**1073–1078.
47. **Nieto-Cerón, S., M. T. Moral-Naranjo, E. Muñoz-Delgado, C. J. Vidal, and F. J. Campoy.** 2004. Molecular properties of acetylcholinesterase in mouse spleen. Neurochem. Int. **45:**129–139.
48. **Nijholt, I., N. Farchi, M. Kye, E. H. Sklan, S. Shoham, B. Verbeure, D. Owen, B. Hochner, J. Spiess, H. Soreq, and T. Blank.** 2004. Stress-induced alternative splicing of acetylcholinesterase results in enhanced fear memory and long-term potentiation. Mol. Psychiatry **9:**174–183.
49. **Nitsch, R. M., B. E. Slack, R. J. Wurtman, and J. H. Growdon.** 1992. Release of Alzheimer amyloid precursor derivatives stimulated by activation of muscarinic acetylcholine receptors. Science **258:**304–307.
50. **Parent, A., D. J. Linden, S. S. Sisodia, and D. R. Borchelt.** 1999. Synaptic transmission and hippocampal long-term potentiation in transgenic mice expressing FAD-linked presenilin 1. Neurobiol. Dis. **6:**56–62.
51. **Parks, A. L., and D. Curtis.** 2007. Presenilin diversifies its portfolio. Trends Genet. **23:**140–150.
52. **Perrier, N. A., M. Salani, C. Falasca, S. Bon, G. Augusti-Tocco, and J. Massoulié.** 2005. The readthrough variant of acetylcholinesterase remains very minor after heat shock, organophosphate inhibition and stress, in cell culture and in vivo. J. Neurochem. **94:**629–638.
53. **Perry, E. K., R. H. Perry, G. Blessed, and B. E. Tomlinson.** 1977. Necropsy evidence of central cholinergic deficits in senile dementia. Lancet **i:**189.
54. **Podlisny, M. B., M. Citron, P. Amarante, R. Sherrington, W. Xia, J. Zhang, T. Diehl, G. Levesque, P. Fraser, C. Haass, E. H. Koo, P. Seubert, P. St George-Hyslop, D. B. Teplow, and D. J. Selkoe.** 1997. Presenilin proteins undergo heterogeneous endoproteolysis between Thr291 and Ala299 and occur as stable N- and C-terminal fragments in normal and Alzheimer brain tissue. Neurobiol. Dis. **3:**325–337.
55. **Popescu, B. O., A. Cedazo-Minguez, E. Benedikz, T. Nishimura, B. Winblad, M. Ankarcrona, and R. F. Cowburn.** 2004. Gamma-secretase activity of presenilin 1 regulates acetylcholine muscarinic receptor-mediated signal transduction. J. Biol. Chem. **279:**6455–6464.
56. **Probst, A., D. Langui, and J. Ulrich.** 1991. Alzheimer's disease: a description of the structural lesions. Brain Pathol. **1:**229–239.
57. **Puelles, E., D. Acampora, R. Gogoi, F. Tuorto, A. Papalia, F. Guillemot, S. L. Ang, and A. Simeone.** 2006. Otx2 controls identity and fate of glutamatergic progenitors of the thalamus by repressing GABAergic differentiation. J. Neurosci. **26:**5955–5964.
58. **Qian, S., P. Jiang, X. M. Guan, G. Singh, M. E. Trumbauer, H. Yu, H. Y. Chen, L. H. Van de Ploeg, and H. Zheng.** 1998. Mutant human presenilin 1 protects presenilin 1 null mouse against embryonic lethality and elevates Aβ1-42/43 expression. Neuron **20:**611–617.
59. **Queralt, R., M. Ezquerra, A. Lleó, M. Castellví, J. Gelpí, I. Ferrer, N. Acarín, L. Pasarín, R. Blesa, and R. Oliva.** 2002. A novel mutation (V89L) in the presenilin 1 gene in a family with early onset Alzheimer's disease and marked behavioral disturbances. J. Neurol. Neurosurg. Psychiatry **72:**266–269.
60. **Rees, T., P. I. Hammond, H. Soreq, S. Younkin, and S. Brimijoin.** 2003. Acetylcholinesterase promotes beta-amyloid plaques in cerebral cortex. Neurobiol. Aging **24:**777–787.
61. **Rees, T. M., A. Berson, E. H. Sklan, L. Younkin, S. Younkin, S. Brimijoin, and H. Soreq.** 2005. Memory deficits correlating with acetylcholinesterase splice shift and amyloid burden in doubly transgenic mice. Curr. Alzheimer Res. **2:**291–300.
62. **Robitzki, A., A. Mack, U. Hoppe, A. Chatonnet, and P. G. Layer.** 1997. Regulation of cholinesterase gene expression affects neuronal differentiation as revealed by transfection studies on reaggregating embryonic chicken retinal cells. Eur. J. Neurosci. **9:**2394–2405.
63. **Rossner, S., U. Ueberham, R. Schliebs, J. R. Pérez-Polo, and V. Bigl.** 1998. The regulation of amyloid precursor protein metabolism by cholinergic mechanisms and neurotrophin receptor signaling. Prog. Neurobiol. **56:**541–569.
64. **Rotundo, R. L.** 1988. Biogenesis of acetylcholinesterase molecular forms in muscle: evidence for a rapidly turning over, catalytically inactive precursor pool. J. Biol. Chem. **263:**19398–19406.
65. **Sáez-Valero, J., G. Sberna, C. A. McLean, C. L. Masters, and D. H. Small.** 1997. Glycosylation of acetylcholinesterase as diagnostic marker for Alzheimer's disease. Lancet **350:**929.
66. **Sáez-Valero, J., G. Sberna, C. A. McLean, and D. H. Small.** 1999. Molecular isoform distribution and glycosylation of acetylcholinesterase are altered in brain and cerebrospinal fluid of patients with Alzheimer's disease. J. Neurochem. **2:**1600–1608.

67. **Sage, H. J., and R. W. Green.** 1972. Common Lentil (*Lens culinaris*) Phytohemagglutinin. Methods Enzymol. **28:**332–339.
68. **Santos, S. C., I. Vala, C. Miguel, J. T. Barata, P. Garção, and P. Agostinho.** 2007. Expression and subcellular localization of a novel nuclear acetylcholinesterase protein. J. Biol. Chem. **282:**25597–25603.
69. **Sberna, G., J. Sáez-Valero, K. Beyreuther, C. L. Masters, and D. H. Small.** 1997. The amyloid β-protein of Alzheimer's disease increases acetylcholinesterase expression by increasing intracellular calcium in embryonal carcinoma P19 cells. J. Neurochem. **69:**1177–1184.
70. **Sberna, G., J. Sáez-Valero, Q. X. Li, C. Czech, K. Beyreuther, C. L. Masters, C. A. McLean, and D. H. Small.** 1998. Acetylcholinesterase is increased in the brains of transgenic mice expressing the C-terminal fragment (CT100) of the beta-amyloid protein precursor of Alzheimer's disease. J. Neurochem. **71:**723–731.
71. **Selkoe, D. J.** 2004. Cell biology of protein misfolding: the examples of Alzheimer's and Parkinson's diseases. Nat. Cell Biol. **6:**1054–1061.
72. **Siman, R., and J. Velji.** 2003. Localization of presenilin-nicastrin complexes and gamma-secretase activity to the trans-Golgi network. J. Neurochem. **84:**1143–1153.
73. **Sklan, E. H., A. Berson, K. R. Birikh, A. Gutnick, O. Shahar, S. Shoham, and H. Soreq.** 2006. Acetylcholinesterase modulates stress-induced motor responses through catalytic and noncatalytic properties. Biol. Psychiatry **60:**741–751.
74. **Sternfeld, M., S. Shoham, O. Klein, C. Flores-Flores, T. Evron, G. H. Idelson, D. Kitsberg, J. W. Patrick, and H. Soreq.** 2000. Excess "read-through" acetylcholinesterase attenuates but the "synaptic" variant intensifies neurodeterioration correlates. Proc. Natl. Acad. Sci. USA **97:**8647–8652.
75. **St. George-Hyslop, P. H.** 2000. Molecular genetics of Alzheimer's disease. Biol. Psychiatry **47:**183–199.
76. **Tandon, A., and P. Fraser.** 2002. The presenilins. Genome Biol. **3:**3014.
77. **Thinakaran, G., D. R. Borchelt, M. K. Lee, H. H. Slunt, L. Spitzer, G. Kim, T. Ratovitsky, F. Davenport, C. Nordstedt, M. Seeger, J. Hardy, A. I. Levey, S. E. Gandy, N. A. Jenkins, N. G. Copeland, D. L. Price, and S. S. Sisodia.** 1996. Endoproteolysis of presenilin 1 and accumulation of processed derivatives in vivo. Neuron **17:**181–190.
78. **Ulrich, J., W. Meier-Ruge, A. Probst, E. Meier, and S. Ipsen.** 1990. Senile plaques: staining for acetylcholinesterase and A4 protein: a comparative study in the hippocampus and entorhinal cortex. Acta Neuropathol. **80:**624–628.
79. **Wolfe, M. S.** 2007. When loss is gain: reduced presenilin proteolytic function leads to increased Aβ42/Aβ40. EMBO J. **8:**136–140.
80. **Wright, C. I., C. Guela, and M. M. Mesulam.** 1993. Protease inhibitors and indoleamines selectively inhibit cholinesterases in the histopathologic structures of Alzheimer disease. Proc. Natl. Acad. Sci. USA **90:**683–686.
81. **Xie, W., J. A. Stribley, A. Chatonnet, P. J. Wilder, A. Rizzino, R. D. McComb, P. Taylor, S. H. Hinrichs, and O. Lockridge.** 2000. Postnatal developmental delay and supersensitivity to organophosphate in gene-targeted mice lacking acetylcholinesterase. J. Pharmacol. Exp. Ther. **293:**896–902.
82. **Zimmermann, M., F. Gardoni, E. Marcello, F. Colciaghi, B. Borroni, A. Padovani, F. Cattabeni, and M. Di Luca.** 2004. Acetylcholinesterase inhibitors increase ADAM10 activity by promoting its trafficking in neuroblastoma cell lines. J. Neurochem. **90:**1489–1499.